Local luminance effect on spatial summation in the foveal vision and its implication on image artifact classification

Chien-Chung Chen[1], San-Yuan Lin[1], Hui-Ya G. Han[1], Sheng-Tzung Kuo[2], Kuo-Chung Huang[3]

1. Department of Psychology, National Taiwan University, Taipei, Taiwan
2. Taiwan TFT LCD Association, Hsinchu, Taiwan
3. The Opto-Electronics and Systems Laboratories, Industrial Technology Research Institute, Hsinchu, Taiwan

ABSTRACT

We investigated the spatial summation effect on pedestals with difference luminance. The targets were luminance modulation defined by Gaussian functions. The size of the Gaussian spot was determined by the scale parameter (standard deviation, σ) which ranged from 0.13° to 1.04°. The local luminance pedestal (2° radius) had mean luminance ranged from 2.9 to 29cd/m^2. The no-pedestal condition had a mean luminance 58cd/m^2. We used a QUEST adaptive threshold seeking procedure and 2AFC paradigm to measure the target contrast threshold at different target sizes (spatial summation curve) and pedestal luminance. The target threshold decreased as the target spatial extent increased with a slope -0.5 on log-log coordinates. However, if the target size was large enough (σ>0.3°), there was little, if any, threshold reduction as the target size further increased. The spatial summation curve had the same shape at all pedestal luminance levels. The effect of the pedestal was to shift the summation curve vertically on log-log coordinates. Hence, the size and the luminance effects on target detection are separable. The visibility of the Gaussian spot can be modeled by a function with a form f(L)*g(σ) where f(L) is a function of local luminance and g(σ) is a function of size.

Key words: Mura pattern, video display, spatial vision, detection threshold, gain control, filtering,

1. INTRODUCTION

Thin-film transistor liquid crystal displays (TFT-LCDs) have been developed for various kinds of displays from computer monitors, television, to cellular phones. However, despite the great improvement in

Human Vision and Electronic Imaging XI, edited by Bernice E. Rogowitz, Thrasyvoulos N. Pappas, Scott J. Daly, Proc. of SPIE-IS&T Electronic Imaging, SPIE Vol. 6057, 605703, © 2006 SPIE-IS&T · 0277-786X/06/$15

manufacturing technology that allows mass production of high quality TFT-LCDs, visible image artifacts on the displays are still commonly seen. These visual artifacts, termed "Mura pattern" in the literature (Mori et al. 2000; Lee et al. 2003; Tamura et al. 2004), are imperfects in the display pixel matrix that are visible when the display is in operation. These artifacts are usually low contrast and blurred luminance modulation.

Currently, the quality control for the visual artifacts is conducted through visual inspection by trained human inspectors. The inspectors classify the displays into categories by the visibility of the artifacts. A procedure of the visual inspection uses the phenomenon that the contrast detection threshold of the Mura patterns decreases with the display luminance (Lee et al. 2003). In this procedure, the inspectors use a set of neutral density (ND) filters to reduce the luminance around the Mura pattern without changing its contrast. Since the visibility of the Mura pattern decreases with luminance, a denser ND filter can render a higher contrast Mura pattern undetectable than a less dense one. Hence, the visibility of the Mura pattern can be determined by the transmittance rate of the most opaque ND filter with which the Mura pattern is detectable.

This procedure is not perfect. Due to the difference in training, policy or measurement apparatus, the artifact classification result may be different from a company to another. The purpose of this study was to establish a standard metrics for Mura pattern visibility such that the visual inspection results from different companies and inspectors can be compared. We considered two variables that might affect Mura pattern detection: Size and luminance.

The visibility of a reasonable small visual stimulus increases with its area. In general, the detection threshold to a visual target decreases as its size increases up to a critical value. Beyond this critical value, a further increase in size produces little, if any, threshold decrement (Barlow, 1958; Howell & Hess, 1978; Robson & Graham, 1981; Watson et al. 1983; Polat & Tyler, 1999). In the literature, the critical size has been considered as reflecting the spatial extent of the receptive field of the target detecting mechanisms (Watson et al., 1983; Daugman, 1985). Since the response of a target detecting mechanism to a visual stimulus is determined by the stimulus strength within its receptive field, using stimulus size to probe the receptive field is important in our modeling.

There are many studies on luminance effects on pattern detection. It is long known that the luminance threshold of a disk stimulus increases as the background luminance increases (e.g., Aguilar & Stiles, 1954; Yang, Qi & Makous, 1995). The typical result was that, as long as the background luminance was greater than a certain value, termed the "dark light", the luminance threshold increased with background luminance

linearly on log-log coordinates. This linear relationship covered a range of 10000-fold background luminance increment from the dark light and was often modeled Weber's law which states that luminance threshold is proportional to background luminance or $\Delta I/I = k$ where ΔI is the luminance threshold, I is the background luminance and k is a constant. A more general model would have luminance threshold as a power function of background luminance or $(\Delta I/I)^p = k$ where is p is an exponent parameter (Barlow, 1958). Using periodic patterns as stimuli, it was reported, Luminance contrast threshold, however, decreases with background luminance (Van Nes & Bouman, 1967). These previous results, however, may not be applied in our modeling effort. In those studies, the visual targets were presented on a large background which provided an adaptation point for the visual system. In this study, the local luminance change created by the ND filters was immediately around the target. Both the target and the ND filters were surrounded by a large and bright background – the display itself. It is not clear whether Weber's law is still hold in our case. Given that the inspectors can reduce the visibility of the Mura patterns by using more opaque ND filters and that the ND filters do not change the physical contrast which is often defined as $(\Delta I/I)$, the detection threshold does not follow Weber's law. Hence, we need a measurement to determine the relationship between local luminance and target visibility.

We measured the detection threshold of simulated Mura patterns with different size and different ND filter transmittance rate to characterize how the visibility of the Mura pattern depends on these two variables. With those data and known properties of human spatial vision, we constructed a model for Mura pattern visibility. This model, in turn, provides a base for a standard metric for Mura patterns.

2. METHOD

2.1 Stimulus.

Since Mura patterns are often characterized as a gradual change of luminance with certain area, we used spots defined by a two-dimensional Gaussian function as our target stimulus. The size of the visual target was defined by the scale parameter ("standard deviation"), σ, of the Gaussian function. That is,

$$M(x, y) = L_o * ((1+c) * \exp(-(x^2/2\sigma^2) * \exp(-(y^2/2\sigma^2)). \quad (1)$$

where L_o is the local background luminance and c is the contrast. We used scale parameter in the range from 0.13 degree to 1.04 degree visual angle in our experiment for all but one observer who was tested in the range from 0.13 degree to 2.08 degree visual angle. The overall luminance of the display was 58 cd/m^2. The local luminance was modified by ND filters with 2 degree radius. The transmittance rate of the ND filters was 50%, 10%, 5% which reduced the local mean luminance to 29, 5.8, and 2.9 cd/m^2. Thus, there were four local luminance conditions: one no-ND filter condition and three ND filter conditions.

2.2 Apparatus.

The display was a TFT-LCD monitor controlled by an IBM PC compatible computer. The observers were placed in front of the monitor with their heads stabilized by a chin rest. The viewing distance was 51 cm. At this distance, the size of each pixel was 2' visual angle and the size of the display was 34.1^{o} by 42.7^{o} visual angle. The mean luminance of the display was 59 cd/m^2. The monitor was calibrated by a Lightmouse (Tyler, 1997) photometer and the gamma function was linearized by a custom software.

2.3 Procedure.

We used a temporal two-alternative forced-choice paradigm to measure the target threshold. The duration of each interval was 90 ms. The time interval from the offset of the first stimulus to the offset of the second stimulus was 800ms. In each trial, the target was randomly presented in either one of the intervals. The task of the observer was to determine which interval contained the target. We used a QUEST adaptive threshold seeking algorithm (Watson & Pelli, 1984) to measure the threshold for each stimulus size and local luminance. Four naïve observers participated in this study. None of the observers received training as visual inspectors in the factory. All observers have normal or corrected to normal visual acuity.

3. RESULT AND DISCUSSION

3.1 Spatial summation

Figure 1 shows how the detection threshold changed with target pattern spatial extent in four naïve observers when there was no ND filter applied. This function which relates detection threshold and the pattern spatial extent is called spatial summation function in this paper. The abscissa denotes the spatial extent of the Gaussian target pattern. We used the scale parameter of the Gaussian function in degree visual angle for spatial extent. Note that the spatial extent is the length of the test pattern in either the x or y dimension. The area of the target pattern is proportional to the square

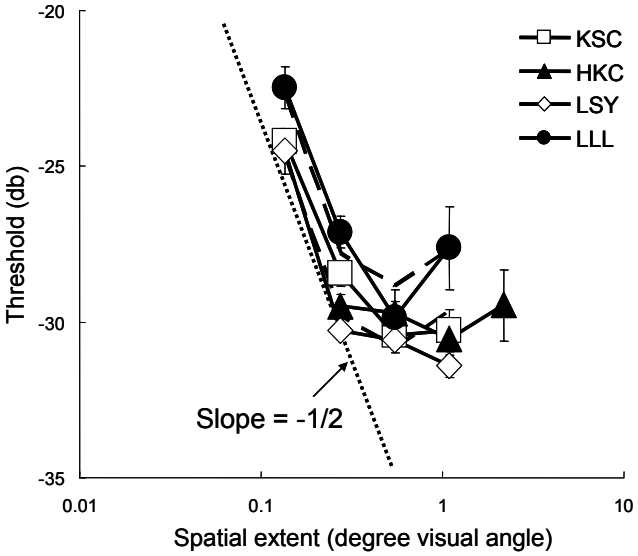

Figure 1. Spatial summation curves for four naïve observers. Most data points are within the +/-1dB range of the mean (bold dashed curve). When the pattern size is small, the threshold decreases with size with a slope -1/2 (dotted line)

of the spatial extent. The ordinate denotes the detection threshold. The unit of the detection threshold is dB (decibel) which is 20 times the log base 10 of the percentage contrast. When the pattern was small, the detection threshold decreased with pattern spatial extent with a slope -1/2 (shown as the thick doted line in Figure 1) on log-log coordinates. That is, the threshold decreased with area with a slope -1/4. However, if the pattern was large enough, there was little, if any, threshold reduction as the pattern spatial extent further increased. As a result, the spatial summation curve leveled out as the right end of the curves. Our data shows a great consistence among naïve observers. The bold dashed curves denote the +/- 1 dB boundary from the mean threshold at each pattern size. Most data are within this boundary. Since the precision of the apparatus was 1dB, it can be concluded that there was practically no significant individual difference. Hence, in the following figures and discussion, we will only show the thresholds averaged across the observers.

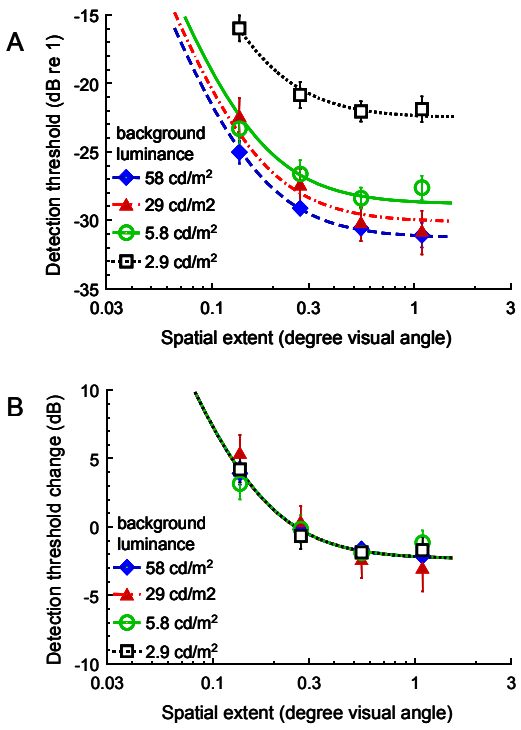

Figure 2. (A) Spatial summation curves at different local background luminance from 58 cd/m^2 (diamond, dashed curve), 29 cd/m^2 (triangle, dash-dot curve), 5.8 cd/m^2 (circle, solid curve) to 2.9 cd/m^2 (square, dotted curve). The smooth curves are the fit of the reduced pattern vision model discussed in the text. (B) The same data as in (A) but each point is scaled by the mean of thresholds measured in each background luminance condition.

3.2 Local luminance effect

Figure 2 (A) shows how spatial summation curves under different ND filter transmittance rate. Hence, it shows how summation curves change with local luminance. The smooth curves are the fits of the model that will be discussed below. The spatial summation curves had the same shape across all local luminance conditions for all observers. The threshold decreased as the target size increased with a slope of -0.5 on log-log coordinates from 0.13 degree to about 0.3 degree and kept constant as the size further increased. That is, all the spatial summation curves had the same shape under all the local luminance conditions. The effect of local luminance is to shift the spatial summation function vertically on a log-log plot. Figure 2(B) shows the same data as in the Figure 2(A) scaled by the mean threshold of the respective curve. It is obvious that all the spatial summation functions overlap with each other after this scaling.

3.3 The model

We fit a reduced version of a pattern vision model (Foley & Chen, 1997) to the data. The first stage of the model is a spatial linear filter that emulates the receptive field of the primary visual cortical cells. The excitation of this linear filter is the product of the sensitivity profile of the linear filter and the input image pattern integrated over space. Let f(x, y) be the sensitivity of the linear filter at position (x, y) and m(x, y) be the luminance modulation from background produced by the input image (a Mura pattern in our case). The input image pattern in this study was defined by a two-dimensional Gaussian function. That is, from Eq. (1), removing the effect of DC component.

$M(x, y) = c * \exp(-(x^2/2\sigma^2) * \exp(-(y^2/2\sigma^2)$.

where σ is the scale parameter of the Gaussian function and c is the contrast of the input image pattern.

The excitation of the linear filter E is

$$E = \int_{-\infty}^{\infty} M(x,y) \bullet f(x,y)\,dxdy \qquad (2)$$

We assume that the sensitivity profile of the linear filter is also a two-dimensional Gaussian with scale parameter s instead of σ. Hence Eq. (2) becomes

$$E = c\int_{-\infty}^{\infty} \exp(-x^2/2\sigma^2)\exp(-y^2/2\sigma^2) \bullet \exp(-x^2/2s^2)\exp(-y^2/2s^2)\,dxdy$$

$$= c(2\pi(\frac{s^2\sigma^2}{s^2+\sigma^2})) \qquad (3)$$

In a full model of pattern vision mechanism, there will be a nonlinear operation on E to get the response R of the mechanism. The detection threshold occurs when R reaches a certain criterion. The

nonlinear response is given (Foley & Chen, 1997) as

$$R = E^p / I^q + z \quad (4)$$

where I is also a power function of c which is called divisive inhibition on the literature; p and q are the exponent of E and I respectively and z is an additive constant that controls the dynamic range of the response function R. The threshold occurs when R reaches a constant. For the convenience of computation, this constant is scaled to 1.

However, near threshold, the inhibition term I^q is much smaller than z. hence, its effect is negligible. Eq, (4) at threshold can simplified as

$$R = 1 = E^p/z \quad (5)$$

Plug Eq (3) into Eq (5), at threshold, we should have

$$Z^{1/p} = c_t * 2\pi *(s^2\sigma^2/(s^2+\sigma^2))$$

Or

$$c_t = g' * ((s^2+\sigma^2)/s^2\sigma^2)) \quad (6)$$

where c_t is the threshold, $g' = Z^{1/p}/2\pi$ is the parameter to be estimated.

There were two free parameters to be estimated in this model: the scale parameter of the linear filter s and the weighting parameter g'. The parameter s is the same for all conditions while g' was allowed to vary with the ND filter transmittance rate. This model fits the data well. The RMSE were only 0.59 dB which is very close to the averaged standard deviation of 0.6 dB.

Table 1. Parameter values of the reduced pattern vision model

s (degree)	0.15
g'	
Luminance (cd/m^2)	
57	0.000558
28.5	0.000637
5.7	0.000742
2.9	0.001531

Table 1 shows the fitted parameter values. The scale parameter of the receptive field was 0.15 degree. The weighting parameter g' is a power function of local luminance and hence a linear function on a log-log plot. The best fitting function is $0.0016*L^{-0.2826}$, where L is the mean luminance of the ND filtered Mura pattern.

Plug in the parameter values back in the model, the visibility of the simulated Mura pattern is inversely proportional to

$$T=(0.0016*L^{-0.2826}) * ((0.0225+\sigma^2)/0.0225^2\sigma^2)) \quad (7)$$

where L is the background luminance and σ is the spatial extent of simulated Mura pattern. The metrics T hence provides a way to compare the visibility of the Mura patterns once their size and the local luminance at threshold are known.

4. CONCLUSION

The spatial extent of the receptive field of the target detection mechanism does not change with mean luminance level. As a result, the spatial summation behavior is the same for all mean luminance level tested. The local luminance effect can be accounted for by the change in a gain parameter that is a linear function of local luminance level on log-log coordinates, that is, a power function of local luminance. Hence, the size and the luminance effects on pattern detection are separable. The visibility of the Mura pattern can be modeled by a function with a form $f(L)*g(\sigma)$ where $f(L)$ is a power function of local luminance and $g(\sigma)$ is a function of size. This function provides a way to compare artifact visibility across different local luminance conditions.

ACKNOWLEGEMENT

Sponsored by a TTLA (Taiwan TFT LCD Association) grant 94E2017 to CCC.

REFERENCES

Aguilar, M. & Stiles, W. S. (1954). Weber's law and saturation of rods. *Optica Acta*, **1**, 54.

Barlow, H. B. (1958). Temporal and spatial summation in human vision at different background intensity. *Journal of Physiology*, **141**, 337-350.

Foley, J. M. & Chen C.C. (1997). Analysis of the effect of pattern adaptation on pattern pedestal effect: A two-process model. *Vision Research*, **37**, 2779-2788.

Howell, E. R., & Hess, R. F. (1978). The functional area for summation to threshold for sinusoidal gratings. *Vision Research*, **18**, 369-374.

Lee, D., Kim, I. Jeong, M. C., Oh, B. K. & Kim, W. Y. (2003). Mura analysis method by using JND luminance and SEMU definition. *Proceeding of the 10th International Display Workshop*, 1467-1470.

Mori, Y., Tanahashi, K. , Tsuji, S. (2000). Quantitative evaluation of visual performance of liquid crystal displays. *Proceedings of SPIE*, **4113**, 242-249.

Polat, U., & Tyler, C.W. (1999). What pat-tern the eye sees best. *Vision Research*, **39**, 887-95.

Robson, J. G., & Graham, N. (1981). Probability summation and regional variation in contrast sensitivity across the visual field. *Vision Research*, **21**, 409-418.

Tamura, T., Tanaka, K., Baba, M., Suzuki, M. and Furuhata, T. (2004). Just Noticeable Difference(JND) Contrast of "Mura" in LCDs on the Five Background Luminance Levels. *Proceeding of the 11th International Display Workshop*, 1527-1530.

Tyler, C. W. (1997) The Morphonome image psychophysics software and a calibrator for Macintosh systems. *Spatial Vision*, **10**, 479-484.

Van Nes, F. L. & Bouman, M. A. (1967). Variation of contrast sensitivity with luminance. *Journal of the Optical Society of America,* **57**, 401-6.

Watson A.B., Barlow H.B. & Robson J.G. (1983). What does the eye see best? *Nature*, **302**, 419-22.

Yang, J. Qi, X. & Makous, W. (1995). Zero frequency masking and a model of contrast sensitivity. *Vision Research*, **35**, 1965-1978.